

Quantum annealing-based structural optimization with a multiplicative design update

Naruethep Sukulthanasorn^{1,*}, Junsen Xiao², Koya Wagatsuma², Shuji Moriguchi¹, and Kenjiro Terada¹

¹International Research Institute of Disaster Science, Tohoku University, Aza-Aoba, 468-1, Aramaki, Aoba-ku, Sendai 980-8572, Japan

²Department of Civil and Environmental Engineering, Tohoku University, Aza-Aoba, 468-1, Aramaki, Aoba-ku, Sendai 980-8572, Japan

*naruethep@tohoku.ac.jp

ABSTRACT

This paper presents a new structural design framework, developed based on iterative optimization via quantum annealing (QA). The novelty lies in its successful design update using an unknown design multiplier obtained by iteratively solving the optimization problems with QA. In addition, to align with density-based approaches in structural optimization, multipliers are multiplicative to represent design material and serve as design variables. In particular, structural analysis is performed on a classical computer using the finite element method, and QA is utilized for topology updating. The primary objective of the framework is to minimize compliance under an inequality volume constraint, while an encoding process for the design variable is adopted, enabling smooth iterative updates to the optimized design. The proposed framework incorporates both penalty methods and slack variables to transform the inequality constraint into an equality constraint and is implemented in a quadratic unconstrained binary optimization (QUBO) model through QA. To demonstrate its performance, design optimization is performed for both truss and continuum structures. Promising results from these applications indicate that the proposed framework is capable of creating an optimal shape and topology similar to those benchmarked by the optimality criteria (OC) method on a classical computer.

Introduction

Quantum computing has attracted a great deal of attention as a solution method for optimization problems because it can take advantage of the unique capabilities of quantum mechanics. One of the leading algorithms is quantum annealing (QA)¹⁻³, building upon the simulated annealing (SA) algorithm that is used in classical computers. The key advantage of QA is that it uses the quantum tunneling effect to penetrate barriers in the objective function landscape. As a result, the process of searching for an optimal solution is greatly accelerated^{4,5}. It should be noted here that despite its robust performance, QA faces several challenges due to the limitations of current quantum hardware and thus has not yet reached its full potential. In the past decades, however, quantum computer technology has made remarkable progress, especially since the practical application of quantum engines (e.g., D-Wave device^{6,7}, Fujitsu Digital Annealer⁸, Hitachi CMOS Annealing Machine⁹, Toshiba Simulated Bifurcation Machine¹⁰, and Fixstars Amplify Annealing Engine¹¹). This advancement has not only broadened the range of feasible applications but also increased interest in exploration in a variety of fields¹²⁻¹⁶.

Structural optimization is one of the most attractive applications because of its robustness and versatility for various industrial sectors. The obtained results serve as a blueprint for prototyping, but efficiency and performance depend on the chosen method. As a result, various optimization algorithms have been developed, including gradient-based methods^{17,18}, SA^{19,20}, Genetic Algorithms^{21,22}, Harmony Search²³, and Evolutionary Structural Optimization^{24,25}. In the effort to enhance optimization techniques, QA, known for its robustness in solving optimization problems, has emerged as a promising candidate for achieving optimized structures¹⁵. So far, however, there have been relatively few studies in the literature on the application of QA for structural optimization. For example, Will and Chen^{26,27} have explored a truss optimization problem using the D-Wave quantum annealer. In their approach, the structural analysis is conducted by finite element (FE) analysis with a classical computer and then QA is used to search for incremental updates to the sectional area. Their results demonstrate the feasibility of using QA to search for optimized cross sections but are limited to nine truss members. Sato et al.^{28,29} proposed a quantum optimization framework for a simple heat path design of a discrete truss structure with three and five edges, for which the objective function is to minimize the temperature of the target node. In addition, in their approach, both structural analysis and optimization are performed by the variational quantum algorithms in noisy intermediate-scale quantum (NISQ) devices. While these studies have successfully applied QA to simple discrete truss problems, their scale and areas of application remain limited.

Recently, Ye et al.³⁰ developed a topology optimization method using QA, tailored for continuum structure design. In their approach, structural analysis is initially conducted on a classical computer. Subsequently, a hybrid of classical computing and QA is employed to solve optimization problems, adopting a decomposition and splitting strategy to manage complexity. This strategy reformulates the original optimization problem into a series of mixed-integer linear programs (MILPs). They demonstrate this method by designing the Messerschmitt-Bolkow-Blohm (MBB) beam. Although the speed of this method has not yet surpassed classical computers, its application provides significant evidence of the QA's potential in structural optimization.

In the present paper, we propose a new quantum annealing-based optimization framework with a multiplicative update scheme for structural design. First, a QA-based optimizer is proposed by adopting the product of the QA iterative solutions as the design variable for each finite element, which characterizes the present multiplicative update scheme. Second, we develop the QUBO model that aims to minimize compliance while integrating inequality constraints through a penalty method and slack variable. The derived model is suitable for QA and allows the multiplicatively updated design variable to converge to the optimum solution, creating an optimal structure. Lastly, the robustness of the proposed framework was demonstrated by applying it to the design of truss and continuum structures, ensuring its reliability and flexibility.

Optimization framework setting

First, we introduce an update multiplier for updating an elemental design variable, denoted as α , within the FE framework. The value of α lies between $0 \leq \alpha \leq \Theta$, where Θ represents the maximum allowable change value. At each design iteration, the update multiplier value is obtained as the solution to the optimization problem via QA, so that the general stiffness is updated at the i -th design iteration as

$$K^i = \alpha^i \cdot K^{i-1} \quad \text{with} \quad 0 \leq \alpha \leq \Theta, \quad (1)$$

which is considered as an effective stiffness for the optimization problem of interest. In particular, if $\alpha = 0.5$, this iteration means a 50% reduction in the value of K . Conversely, if $\alpha = 1.1$, it means increasing the value of K by 10%. Through this process, the structural layout is dynamically adjusted, with unnecessary areas being reduced and more critical areas being reinforced. It should be noted that the updater α in Eq. (1) is employed solely to update the effective stiffness from the design iteration $(i - 1)$ to i -th. For the structural design layout at each design iteration, it is represented by an additional variable, namely design variable α^* , which can be obtained through the multiplication of all previous updaters α^i as

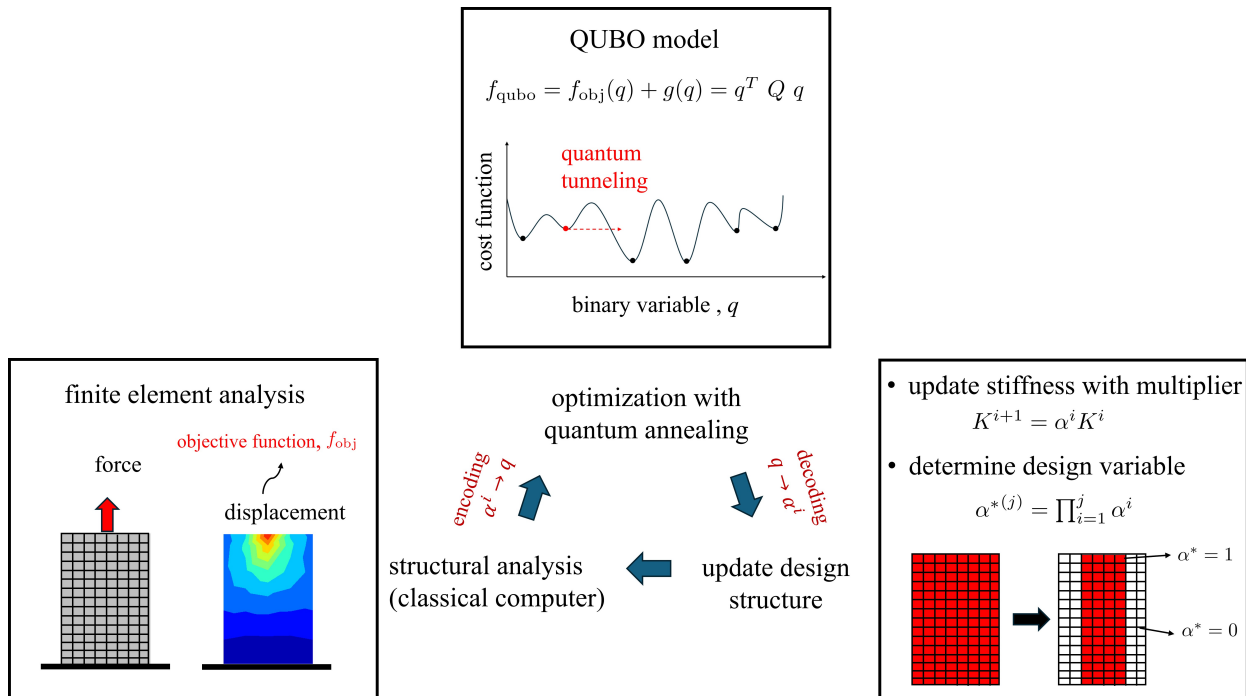


Figure 1. Proposed design framework using quantum annealing-based optimizer.

$$\alpha^{*(j)} = \prod_{i=1}^j \alpha^i \quad \text{with} \quad K^j = \alpha^{*(j)} K^0, \quad (2)$$

where K^0 and K^j are the stiffness at the initial and j -th iterations, respectively. Here, it can be seen from Eqs. (1) and (2) that the value of α^* can increase until it exceeds the specified upper bound. Therefore, a truncation procedure is needed to address this problem so that the limit value is not exceeded. In this study, when the value of design variable α^* in the current design iteration approaches the limit value, Θ is set to 1, prohibiting the alpha value from increasing. In addition, it is worthwhile to notice that α^* is equivalent to the design variable from density-based approaches (e.g., the SIMP method¹⁸). Thus, in a similar fashion, α^* can be used to represent the design material as

$$\alpha^* = \begin{cases} 1 & : \text{solid} \\ 0 < \alpha^* < 1 & : \text{mixture} \\ 0 & : \text{void} \end{cases} . \quad (3)$$

Thanks to the above setting, an optimization problem is established to find a design layout that achieves the target performance. In this study, the objective function is set to minimize the compliance of the structure while incorporating the material volume as the constraint. This is well-known as the standard framework for structural optimization. Once the solution is obtained, the design structure is expected to perform better than the initial design. According to this, the optimization problem can be formulated in the standard form as follows:

$$\begin{aligned} \text{find : } & \boldsymbol{\alpha}^*(\alpha_e) \in \{\alpha_1^*, \alpha_2^*, \dots, \alpha_{N_e}^*\} \quad \text{with Eq. (2)} \\ \text{min : } & \mathbf{F}^T \mathbf{U} \\ \alpha^*(\alpha_e) & \\ \text{s.t. : } & \mathbf{K}(\boldsymbol{\alpha}^*) \mathbf{U} = \mathbf{F}, \\ & \sum_{e=1}^{N_e} \frac{V_e(\alpha_e^*)}{V_0} \leq \bar{V}_{\text{target}}, \quad 0 \leq \alpha_e \leq \Theta, \quad 0 \leq \alpha_e^* \leq 1, \end{aligned} \quad (4)$$

where \mathbf{K} is the global stiffness matrix, \mathbf{F} is the external applied load vector, \mathbf{U} is the global nodal displacement vector in structural analysis. Also, α_e is the elemental update multiplier, N_e is the number of finite elements (or truss members), $V_e(\alpha_e^*)$ is the elemental volume at each design iteration, V_0 is the initial total volume, and \bar{V}_{target} is a given desired ratio to the initial volume. In addition, $\boldsymbol{\alpha}^* = \{\alpha_1^*, \dots, \alpha_{N_e}^*\}$ is the set of design variables. Here, once the optimization is established, then it will be solved for the update multiplier, α , via QA. The overall steps of the proposed design framework can be summarized as follows:

1. Perform structural analysis using the finite element method (FEM) on a classical computer to obtain basic unknowns (e.g., displacements), and then calculate the elemental objective function.
2. Establish the QUBO model by encoding the updaters α_e , which multiplicatively update the elemental design variables α_e^* , into binary variables, transforming the original objective function and the volume constraint to the cost function into the QUBO formats.
3. Solve the QUBO cost function for the updaters α_e using QA.
4. Decode the binary variables back to real values and update the current design structure with α_e and then determine the design variable α_e^* with Eq. (2).

This process is repeated until convergence to an optimal solution is achieved within a predetermined tolerance. The schematic of the proposed framework is shown in Fig. 1.

Methods

This section provides details on converting the optimization problem from the previous section into a QUBO format. A key process for solving the optimization with QA is to derive a combinatorial optimization problem such as the Ising or, equivalently, QUBO model. Details are as follows.

QUBO model

To solve the problem in the QA framework, it is necessary to reformulate the optimization problem in a QUBO format. Depending on each particular problem, the QUBO model, i.e., the cost function, constraints must be derived in the binary variable before passing through a quantum device.

We first define the cost function for the QUBO problem in the following form:

$$f_{\text{qubo}}(\mathbf{q}) = \mathbf{q}^T \cdot \mathbf{Q} \cdot \mathbf{q}, \quad (5)$$

where \mathbf{Q} denotes an upper diagonal coefficient matrix, and q is the unknown binary variable vector whose components are in $q \in \{0, 1\}$. Given the property of binary variables such that $q^2 = q$, Eq. (5) can consequently be reformulated as follows:

$$f_{\text{qubo}}(q) = \sum_{i=1}^n Q_{i,i} q_i + \sum_{i<j}^n Q_{i,j} q_i q_j, \quad (6)$$

where n is the number of qubits, $Q_{i,i}$ and $Q_{i,j}$ are the coefficients of linear and quadratic terms corresponding to the diagonal and off-diagonal entries, respectively. It can be seen that no constraint term appears in Eqs. (5) and (6), implying that the standard QUBO problem is dedicated to an unconstrained optimization problem. However, in structural optimization problems, layouts are usually designed under specific constraints to ensure optimal performance, as presented in Eq. (4). Therefore, in this study, the penalty method is employed to modify the QUBO cost function of the following form:

$$f_{\text{qubo}}(q) = f_{\text{obj}}(q) + \lambda \cdot g(q), \quad (7)$$

where f_{obj} represents the objective function as defined in the structural optimization problem by Eq. (4), g denotes its constraint function, and λ is the positive penalty parameter. Note that the value of λ must be large enough to have an effective impact on the QUBO cost function so that the imposed constraints are satisfied.

It should be noted that since the formulation presented above has been set up as a general design framework, both the objective function and constraint can be customized and tailored to specific applications, thus achieving the desired performance. However, this study focuses on the problems of minimizing structural compliance or equivalently maximizing structural stiffness under the volume constraint. Accordingly, the objective function in Eq. (4) can be expressed using the unknown binary variable q_e for each structural element as follows:

$$f_{\text{obj}}(q_e) = \underbrace{\mathbf{F}^T \mathbf{U}}_{\text{minimizing compliance}} := \underbrace{\mathbf{U}^T \mathbf{K}(\boldsymbol{\alpha}^*(q_e)) \mathbf{U}}_{\text{maximizing stiffness}} \quad (8)$$

Besides, there are two key aspects to be noted for the constraint function $g(q)$. First, the second term on the right-hand side of Eq. (7) is needed only when the equality in Eq. (4) is active, so QA cannot be applied in a QUBO format as it is. To address this issue, an additional variable, known as the slack variable \bar{S} , is introduced into the volume constraint in Eq. (4) as a function of another unknown binary variable q_s . Second, to meet the requirements of the QUBO framework, g is commonly formulated by squaring the volume constraint function to a quadratic form. This modification allows the volume constraint in Eq. (4) to be converted to an equality constraint as

$$\sum_{e=1}^{N_e} \frac{V_e(\boldsymbol{\alpha}_e^*(q_e))}{V_0} - \bar{V}_{\text{target}} + \bar{S}(q_s) = 0, \quad (9)$$

so that the constraint function is defined as

$$g(q_e, q_s) = \left(\sum_{e=1}^{N_e} \frac{V_e(\boldsymbol{\alpha}_e^*(q_e))}{V_0} - (\bar{V}_{\text{target}} - \bar{S}(q_s)) \right)^2. \quad (10)$$

As a result, the optimization framework defined in Eq. (4) can be reformulated by adopting Eqs. (8) and (10) in the QUBO cost function to define the following minimization problem:

$$\begin{aligned} \text{find} & : \quad \boldsymbol{\alpha}^*(q_e) \quad \text{with Eq. (2)} \\ \text{min}_{q_e, q_s} & : \quad f_{\text{qubo}}(q_e, q_s) = -\mathbf{U}^T \mathbf{K}(\boldsymbol{\alpha}^*(q_e)) \mathbf{U} + \lambda \cdot \left(\sum_{e=1}^{N_e} \frac{V_e(\boldsymbol{\alpha}_e^*(q_e))}{V_0} - (\bar{V}_{\text{target}} - \bar{S}(q_s)) \right)^2 \\ \text{with} & \quad \mathbf{K}(\boldsymbol{\alpha}^*(q_e)) \mathbf{U} = \mathbf{F}, \\ & \quad 0 \leq \alpha_e(q_e) \leq \Theta, \quad 0 \leq \alpha_e^*(q_e) \leq 1, \quad 0 \leq \bar{S}(q_s) \leq 1. \end{aligned} \quad (11)$$

It is worth mentioning that the negative value of the first term of f_{qubo} in Eq. (11) arises from the objective of the stiffness of the design structure, and that this expression is identical to the analytical sensitivity formulation in the standard problem of minimizing compliance. Thus, from this perspective, the iterative solving procedure for Eq. (11) with QA can be considered similar to the sensitivity analysis procedure in standard structural optimization.

Encoding

As shown in Eq. (11), the main variables and parameters are represented by binary variables $q \in \{0, 1\}$. Additionally, in the proposed framework, it is important that the value of the updater and slack variable, α_e and \bar{S} , cover a specific range of real numbers in order to effectively update the layout of the design structure. To this end, an encoding procedure using a specific functional form of q is used to represent these real values. For simplicity, a power series expansion of the following form is adopted^{31,32}:

$$\alpha_e(q_e) = \Theta \cdot \left(\sum_{l=-m}^m 2^l \right)^{-1} \cdot \left(\sum_{l=-m}^m 2^l \cdot q_{e,l} \right), \quad \bar{S}(q_s) = \left(\sum_{l_s=-m_s}^{m_s} 2^{l_s} \right)^{-1} \cdot \left(\sum_{l_s=-m_s}^{m_s} 2^{l_s} \cdot q_{s,l_s} \right), \quad (12)$$

where $q_{e,l}$ denotes the unknown binary variable for the l -th basis term of element e , and q_{s,l_s} is the unknown binary variable for the slack variable with the l_s -th basis term. The integers, m and m_s , determine the number of basis terms representing α_e and \bar{S} , respectively. Thus, for element e , the total number of unknown binary variables is $2m$, and for the entire system, it is $2m \cdot N_e + 2m_s$. Notably, the coefficient of each basis consists of two parts, a fractional term and an integer term, which vary depending on whether the powers, l and l_s , are negative or positive. Increasing the values of m and m_s means incorporating more fractional and integer terms, thereby enriching the candidate values of α_e and \bar{S} , respectively. At the same time, however, they also imply an increase in the computational effort required by the quantum machine to search for the values of $q_{e,l}$ and q_{s,l_s} . In this context, the functional form of the encoding is open to debate and will be left for further detailed study.

QUBO formulation for QA machine

The QUBO cost function in Eq. (11) is rearranged as follows:

$$\begin{aligned} f_{\text{qubo}} &= f_{\text{obj}}(q_e) + \lambda \left(\sum_{e=1}^N \frac{V_e(q_e)}{V_0} - (\bar{V}_{\text{target}} - \bar{S}(q_s)) \right)^2 \\ &= f_{\text{obj}}(q_e) + \lambda \left(\left(\sum_{e=1}^N \frac{V_e(q_e)}{V_0} \right)^2 - 2 \left(\sum_{e=1}^N \frac{V_e(q_e)}{V_0} \right) (\bar{V}_{\text{target}} - \bar{S}(q_s)) + (\bar{V}_{\text{target}} - \bar{S}(q_s))^2 \right) \\ &= \underbrace{f_{\text{obj}}(q_e)}_{C_1} + \lambda \left(\underbrace{\sum_{e=1}^N \left(\frac{V_e(q_e)}{V_0} \right)^2}_{C_2} + 2 \underbrace{\sum_{e < j} \left(\frac{V_e(q_e) V_j(q_j)}{V_0^2} \right)}_{C_3} - 2 \underbrace{\left(\sum_{e=1}^N \frac{V_e(q_e)}{V_0} \right) (\bar{V}_{\text{target}} - \bar{S}(q_s))}_{C_4} + \underbrace{(\bar{V}_{\text{target}} - \bar{S}(q_s))^2}_{C_5} \right). \end{aligned} \quad (13)$$

Then, the substitution of Eq. (12) into each term yields

$$C_1 = - \sum_{e=1}^N (\Phi_e) \cdot U_e^T \left(\sum_{l=-m}^m 2^l \cdot q_{e,l} \right) K_e \cdot U_e, \quad (14)$$

$$C_2 = \sum_{e=1}^N (\Phi_e)^2 \left(\sum_{l=-m}^m 2^{2l} \cdot q_{e,l} + \sum_{l < l_2}^m 2^{l+l_2+1} \cdot q_{e,l} q_{e,l_2} \right), \quad (15)$$

$$C_3 = \sum_{e < j}^N \Phi_e \cdot \Phi_j \cdot \left(\sum_{l=-m}^m \sum_{l_2=-m}^m 2^{l+l_2+1} \cdot q_{e,l} \cdot q_{j,l_2} \right), \quad (16)$$

$$C_4 = - \left(\sum_{e=1}^N \Phi_e \cdot \left(\sum_{l=-m}^m 2^{l+1} \cdot q_{e,l} \right) \right) \bar{V}_{\text{target}} + \sum_{e=1}^N \left(\Phi_e \cdot \Phi_s \cdot \left(\sum_{l=-m}^m \sum_{l_s=-m_s}^{m_s} 2^{l+l_s+1} \cdot q_{e,l} q_{s,l_s} \right) \right), \quad (17)$$

$$C_5 = \bar{V}_{\text{target}}^2 - 2 \bar{V}_{\text{target}} \cdot \Phi_s \cdot \left(\sum_{l_s=-m_s}^{m_s} 2^{l_s} \cdot q_{s,l_s} \right) + (\Phi_s)^2 \cdot \left(\sum_{l_s=-m_s}^{m_s} 2^{2l_s} \cdot q_{s,l_s} + \sum_{l_s < l_{s_2}}^{m_s} 2^{l_s+l_{s_2}+1} \cdot q_{s,l_s} q_{s,l_{s_2}} \right), \quad (18)$$

$$\text{and } \Phi_{e,j} = \left(\frac{V_{e,j}}{V_0} \right) \cdot \left(\frac{\Theta}{\sum_{l=-m}^m 2^l} \right); \quad \Phi_s = \left(\frac{1}{\sum_{l_s=-m_s}^{m_s} 2^l} \right).$$

With this QUBO format, the minimization problem in Eq. (11) can be solved using an available QA computing platform. In the present study, the Amplify Annealing Engine (Amplify AE)¹¹, a GPU-based Ising machine, is adopted to search for the ground state of the QUBO problem, with the execution time parameter for the Amplify AE machine, namely t_{out} , set considering the specific problem at hand.

Results and discussion

Truss optimization

First, the proposed framework is applied to the optimal design problem of four truss structures with different geometries and boundary conditions, as shown in Fig. 2. As mentioned before, the state variables (e.g., displacement) are obtained by performing standard structural analysis on a classical computer. In this particular problem, the effective stiffness K stated in Eq. (2) can be a truss member e as $K_e^j = \alpha_e^{*(j)} K_0 = \alpha_e^{*(j)} \cdot E \cdot A_e^0 / L_e$, where $\alpha_e^{*(j)}$ is the elemental design variable at the j -th design iteration, representing the ratio between the current and initial cross-sectional areas, A_e^j / A_e^0 . Here, E is Young's modulus equal to 2×10^6 N/m², L_e is the length and A_e^0 is the initial cross-sectional area equal to 10 mm² for all members. The target ratio \bar{V}_{target} to the initial total volume V_0 is fixed at 1 throughout the optimization process, and the current design volume, denoted by $V_{\text{des}}^j(\alpha^*)$, corresponds to $\sum_{e=1}^{N_e} V_e^j(\alpha_e^*)$ where $V_e^j(\alpha_e^*) = \alpha_e^{*(j)} \cdot A_e^0 \times L_e$.

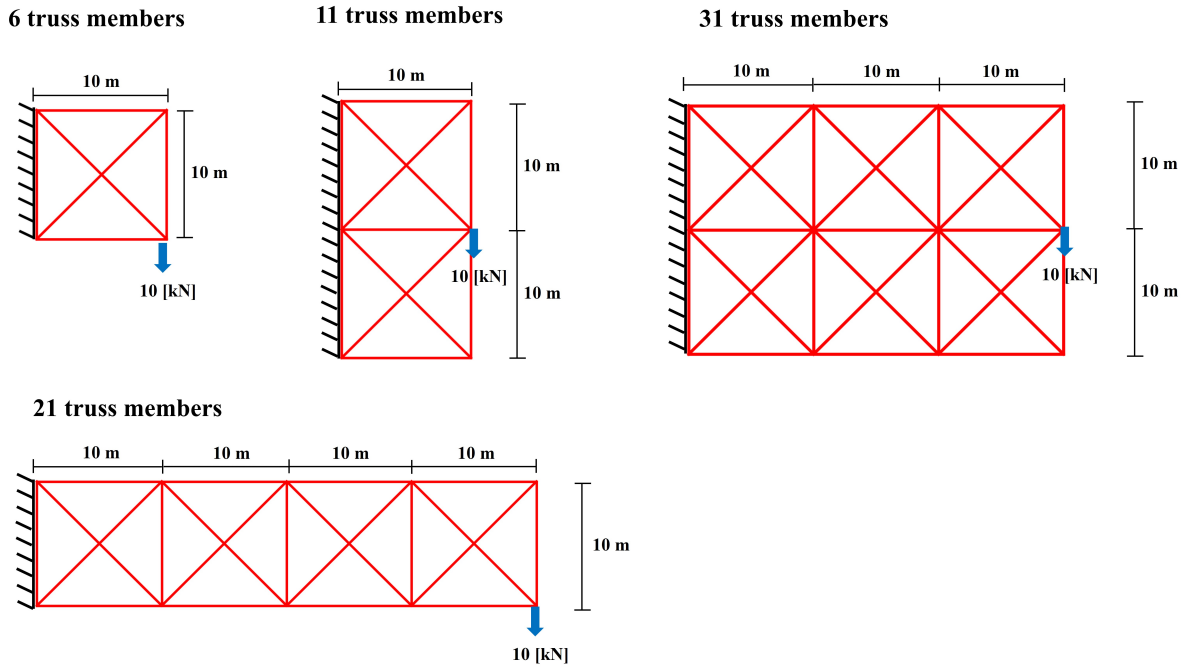


Figure 2. Optimization target: four truss structures with different numbers of members and their support/loading conditions.

Additionally, the number of unknown binary variables is $n = N_e \cdot n_q + n_s$ with n_q and n_s being the numbers of qubits for the elemental updaters and the slack variable, both of which are set to 9 in this study. The execution timeout parameter for the Amplify AE machine is set as $t_{\text{out}} = 5$ seconds for the truss example. Meanwhile, the maximum allowable change Θ can be fixed throughout the optimization process, but we devise a two-step approach to expedite the optimization, in which the initial large value Θ_1 is first set and then reduce to Θ_2 . These values are determined through trial and error for each specific problem, and so are the penalty constant λ . The iterative process for optimization is terminated after the value of the objective function changes by less than 0.005 for five consecutive iterations. For comparison purposes, reference solutions are obtained by the optimality criteria (OC) method¹⁸ performed on a classical computer.

Figure 3 presents the optimization results for the truss structures having 6 and 11 members by setting the penalty parameter λ to 8×10^4 and 5×10^4 , respectively, and the initial design variable $\alpha_e^{*(1)}$ is set to 0.2 for all members. We have set $\Theta_1 = 1.5$ at the first three iterations and $\Theta_2 = 1.05$ for remaining iterations. As can be seen from each of the figures, the objective function

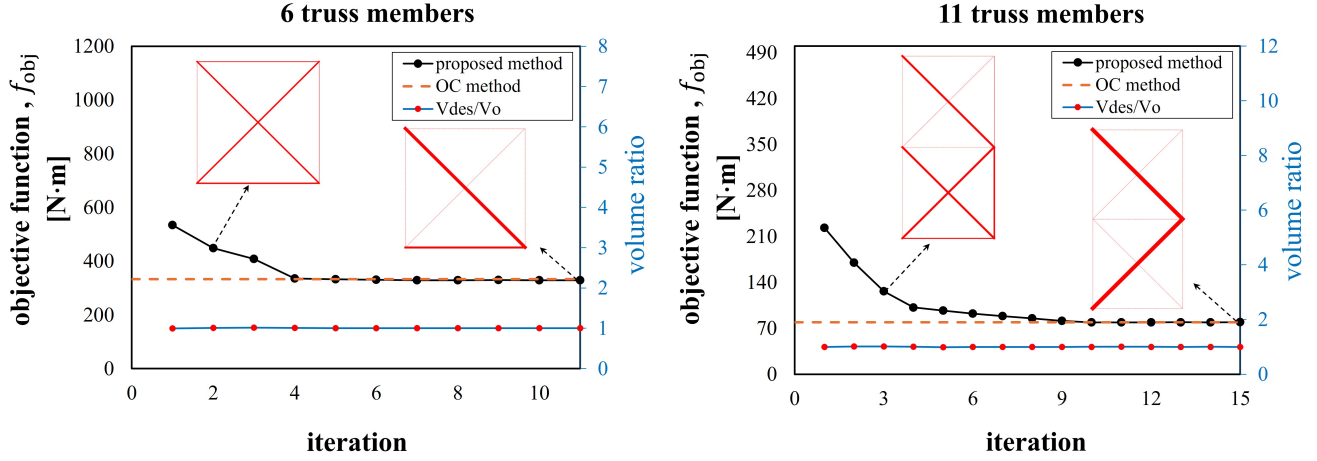


Figure 3. History of truss optimization for 6 and 11 truss members.

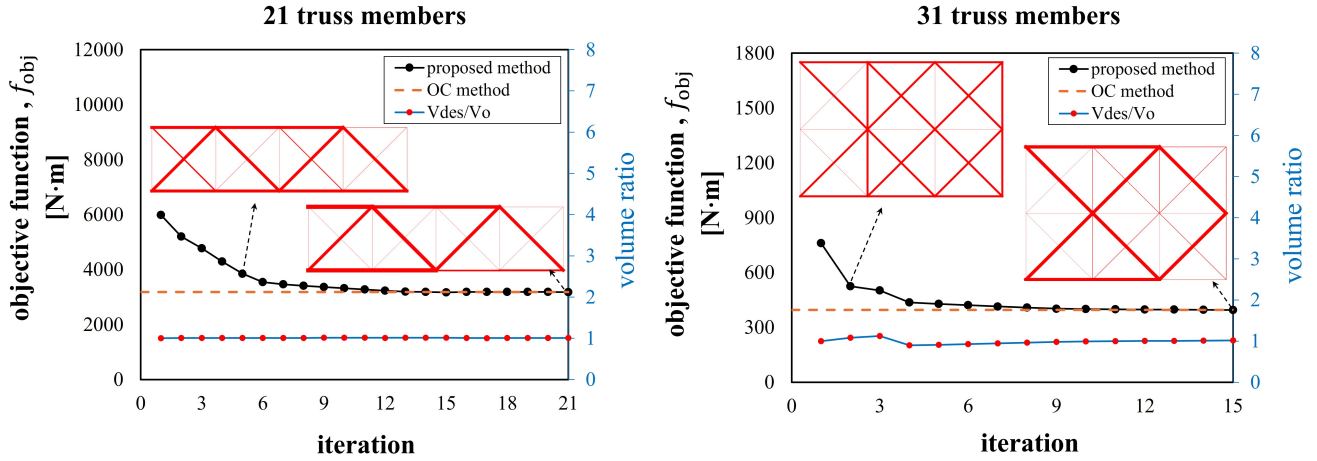


Figure 4. History of truss optimization for 21 and 31 truss members.

value smoothly converges to the optimal solution within a few iterations. Also, the final configuration after convergence is the well-known optimum solution for the two-bar truss problems^{24,26}. Table 1 compares the final values of the objective function and volume ratio obtained from QA and OC methods. As can be seen, for both truss structures, the objective function values obtained from QA are slightly lower than those from the OC method. This is because for each optimization result, the volume ratio to the initial total volume of the optimized truss structure obtained from OA is slightly larger than that from the OC method. It is worthwhile to note that the volume constraint is only approximately satisfied in QA due to two main factors: the value of the penalty constant λ and the precision of the encoding. Improvement of these factors would allow for a more accurate approximation.

Next, we conduct optimization for the two remaining truss structures having 21 and 31 members by setting $\alpha_e^{*(1)} = 0.4$. For the case with 21 members, λ is set to 5.3×10^4 , and Θ_1 is set to 1.15 for the first five iterations, before being reduced to $\Theta_2 = 1.025$. For the case with 31 members, λ is set to 1×10^3 , Θ_1 is set to 1.5 for the first three iterations, and is then reduced to $\Theta_2 = 1.08$. Optimization results are shown in Fig. 4, each from which we can confirm that the objective function converges monotonically to the optimal solution and agrees with that of the OC method. Moreover, the optimized shapes are well-recognized and consistent with the results reported in the literature. Again, the final objective function values are slightly lower than those of the OC method due to the larger values of the final design volume.

It should be pointed out that the encoding parameters (e.g., number of qubits n_q) should be carefully set because the poor encoding may lead to the violation of the volume constraint, as illustrated in this example, and the limited number of possible candidates for the design updater α_e in QA. In other words, the imposition of a certain number of n_q , limits the solution set in

Table 1. Final values of objective function and volume ratio obtained in optimization problems of truss structures.

	6 truss members		11 truss members		21 truss members		31 truss members	
	QA	OC	QA	OC	QA	OC	QA	OC
f_{obj}	328.82	333.08	79.16	79.26	3176.7	3180.6	394.6	395.2
V_{des}/V_0	1.0022	1.0000	1.0005	1.0000	1.0096	1.0000	1.0173	1.0000

QA, which could make α_e in Eq. (12) to potentially overestimate the solution. Nevertheless, the difference in the final objective function value between the OC method and QA remains less than 1.3%.

Continuum structure optimization

In this subsection, we focus our attention on continuum structures made of linearly elastic materials. FE analysis is performed to solve the state variables on a classical computer. Here, the element stiffness matrix in Eq. 2 is calculated as $\mathbf{K}_e^j(\alpha_e^*) = \int_{\Omega_e} \alpha_e^{*(j)} \mathbf{B}^T \mathbf{C}_0 \mathbf{B} dV$, where $\alpha_e^{*(j)}$ represents the ratio between the current and initial elemental volume, V_e^j/V_e^0 , \mathbf{B} is the strain-displacement matrix, Ω_e is the domain of an element, and \mathbf{C}_0 is the elasticity matrix dependent on the material properties. In this study, isotropic elastic properties are taken as $E = 2 \times 10^6 \text{ N/m}^2$ and Poisson's ratio $\nu = 0.3$ under the plane strain condition. Also, for this example, the target ratio \bar{V}_{target} are kept at initial total volume V_0 throughout the optimization process, and $V_e^j(\alpha_e^*) = \alpha_e^{*(j)} \cdot V_e^0$. In order to demonstrate the performance of the proposed framework, two design domains with

Table 2. The final objective function value and its volume for continuum structure optimization.

	coat-hanging		beam with fixed ends	
	QA	OC	QA	OC
f_{obj}	1678.18	1718.51	16370.28	16422.59
V_{des}/V_0	1.0322	1.0000	1.0095	1.0000

different boundary conditions are considered and are discretized with 10×20 and 20×10 elements, respectively, as shown in the leftmost panel of Fig. 5 and Fig. 6. It is important to note that setting the number of n_q in the current available QA machine has limitations, especially when the number of unknowns increases, significantly affecting computational time. Keeping this limitation in mind, n_q and n_s in this example are set to 3 as the small number to explore whether the method will converge or not with $t_{\text{out}} = 1$ second. Additionally, a two-step strategy for Θ is employed again to accelerate the optimization by initially setting Θ_1 for the first three iterations followed by taking a smaller value of Θ_2 . First, we target a well-known coat-hanging problem²⁴ as shown in the leftmost panel of Fig. 5 with $\alpha^{*(1)} = 0.5$, $\Theta_1 = 1.2$, $\Theta_2 = 1.05$, and λ is set to 7×10^3 . The optimized topology and its evolution from the proposed design framework are shown in Fig. 5, along with the optimized result obtained using the OC method. It can be seen from the figure that the QA optimization results closely converge to a topology similar to

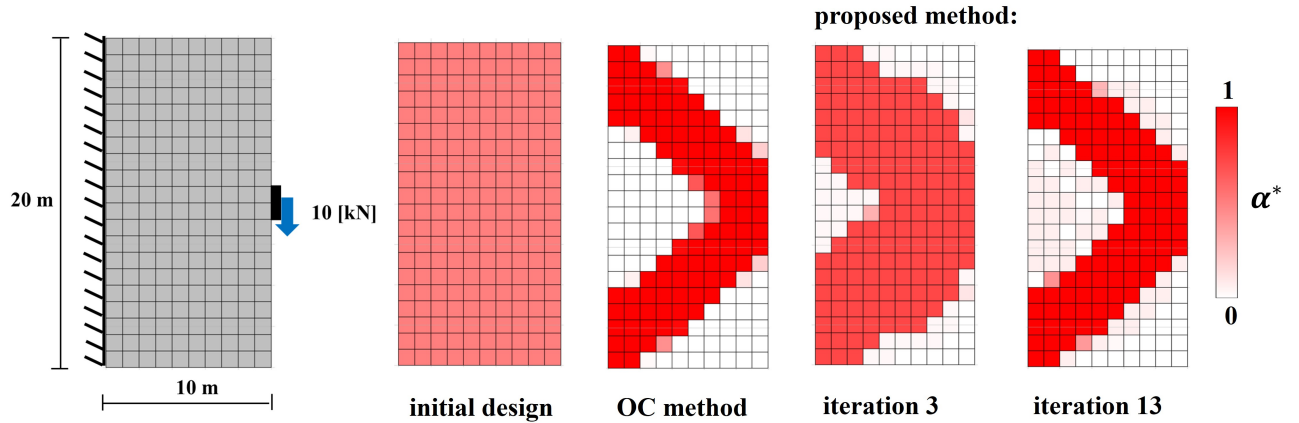


Figure 5. The optimization result for a coat-hanging problem.

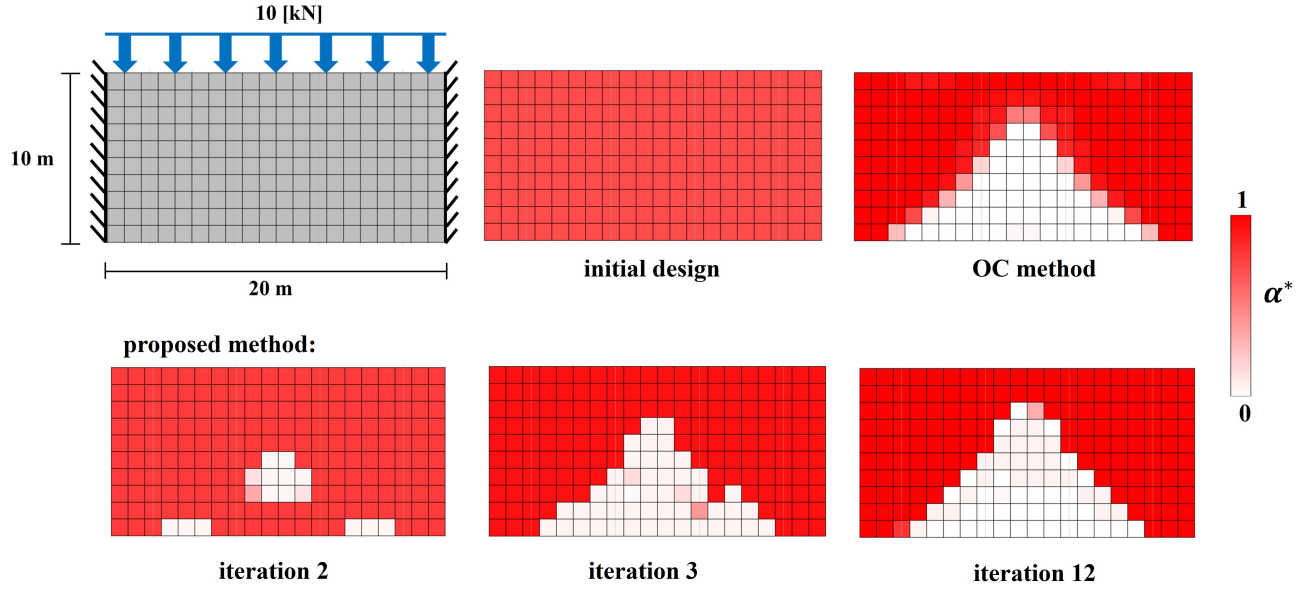


Figure 6. The optimization result for a beam with fixed ends.

the solution of this benchmark problem and that obtained using the OC method. Consequently, it shows that even with a small n_q , convergence to the optimal solution is achievable, implying the reliability and accuracy of using QA in the proposed multiplicative update scheme for structural optimization.

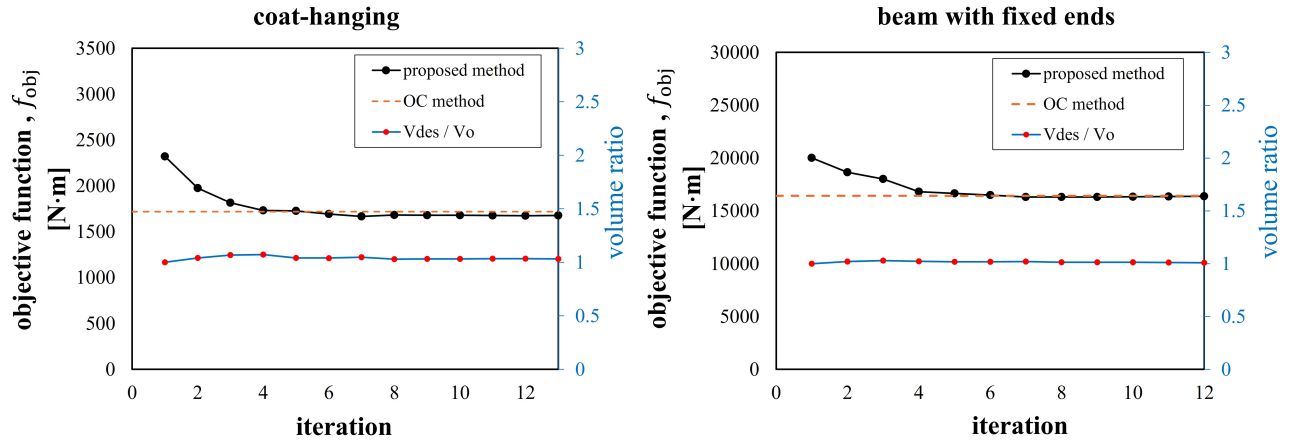


Figure 7. The history of objective function value and its volume for continuum structure optimization.

Next, we consider a beam-like two-dimensional structure with fixed ends as shown in the leftmost panel of Fig. 6. The design parameters are set as follows: $\alpha^{*(1)} = 0.7$, $\Theta_1 = 1.1$, $\Theta_2 = 1.02$, and $\lambda = 1 \times 10^5$. Figure. 6 shows snapshots illustrating the optimization process from the proposed method, which converges to a result similar to the OC method. However, it can be observed that some design variables, α_e^* , obtained from the OC method converge to intermediate values more than those obtained from the proposed method. Although the proposed method tends to clearly split the design variable into 0 or 1, the binary encoding process in Eq. (12), plus the small number of n_q , limited the number of candidate solutions, leading to an overestimation of the design volume, although by less than 4%; see Table 2. Because of this tendency, as in the truss example problems, the final objective function value of the proposed method is slightly lower (less than 2.5%) than that of the OC method.

Nevertheless, the histories of the objective function value and its design volume for both cases shown in Fig. 7 indicate that the optimization results are consistent with the OC method and converge well to the optimal solutions.

Conclusion

We have developed a novel structural design framework based on QA, into which the multiplicative update scheme for the design variable is incorporated. That is, the design variable is represented by the product of updaters, each of which is obtained as a solution provided by QA. The framework is advantageous due to its simplicity and efficiency, which facilitates convergence to the optimal solution. The QUBO form was derived for the compliance minimization problem subject to the inequality volume constraint. A power series expansion encoding process is employed to facilitate the conversion between real and binary values of the updaters so that the design variable of the QUBO model can be updated as their product. This framework has been applied to both truss and continuum structures, demonstrating its robust performance. Indeed, the optimization results indicated that the proposed design framework, utilizing QA, exhibited a good convergence to the optimal design shape for both problems, achieving results comparable to those obtained with the OC method on a classical computer. Remarkably, even with a limited number of binary variables or, equivalently, a small number of qubits, the QA-based design results converged effectively to the optimal solution. However, the final objective function value using QA was lower than that achieved with the OC method, because the design volume was slightly overestimated due to the poor expressive ability of the adopted encoding process and the optimal penalty constant.

It should be noted that the parameters within the proposed framework require fine-tuning for each specific problem, particularly the penalty parameter for imposing the volume constraint in the QUBO model. Therefore, further development is needed to automate the process of finding optimal parameter values. Additionally, exploring alternative functional forms for the encoding process could further increase the efficiency of updating the design variable.

Data availability

The datasets generated and/or analysed during the current study are not publicly available due to an ongoing study but are available from the corresponding author upon reasonable request.

References

1. Kadowaki, T. & Nishimori, H. Quantum annealing in the transverse ising model. *Phys. Rev. E*. **58**, 5355–5363, DOI: [10.1103/PhysRevE.58.5355](https://doi.org/10.1103/PhysRevE.58.5355) (1998).
2. Morita, S. & Nishimori, H. Mathematical foundation of quantum annealing. *J. Math. Physics*. **49**, DOI: [10.1063/1.2995837](https://doi.org/10.1063/1.2995837) (2008).
3. Hauke, P., Katzgraber, H. G., Lechner, W., Nishimori, H. & Oliver, W. D. Perspectives of quantum annealing: Methods and implementations. *Rep. Prog. Phys.* **83**, DOI: [10.1088/1361-6633/ab85b8](https://doi.org/10.1088/1361-6633/ab85b8) (2020).
4. Nishimori, H., Tsuda, J. & Knysh, S. Comparative study of the performance of quantum annealing and simulated annealing. *Phys. Rev. E Stat. Nonlin. Soft Matter Phys.* **91**, DOI: [10.1103/PhysRevE.91.012104](https://doi.org/10.1103/PhysRevE.91.012104) (2015).
5. Albash, T. & Lidar, D. A. Demonstration of a scaling advantage for a quantum annealer over simulated annealing. *Phys. Rev. X*. **8**, DOI: [10.1103/PhysRevX.8.031016](https://doi.org/10.1103/PhysRevX.8.031016) (2018).
6. Mcgeoch, C. & Farré, P. The d-wave advantage system: An overview. Tech. Rep., D-Wave Quantum Systems Inc. (2020).
7. Johnson, M. W. *et al.* Quantum annealing with manufactured spins. *Nature*. **473**, 194–198, DOI: [10.1038/nature10012](https://doi.org/10.1038/nature10012) (2011).
8. Aramon, M. *et al.* Physics-inspired optimization for quadratic unconstrained problems using a digital annealer. *Front. Physics*. **7**, DOI: [10.3389/fphy.2019.00048](https://doi.org/10.3389/fphy.2019.00048) (2019).
9. Yamaoka, M., Okuyama, T., Hayashi, M., Yoshimura, C. & Takemoto, T. Cmos annealing machine: an in-memory computing accelerator to process combinatorial optimization problems. In *2019 IEEE Custom Integrated Circuits Conference (CICC)*, 1–8, DOI: [10.1109/CICC.2019.8780296](https://doi.org/10.1109/CICC.2019.8780296) (IEEE, 2019).
10. Goto, H., Tatsumura, K. & Dixon, A. R. Combinatorial optimization by simulating adiabatic bifurcations in nonlinear hamiltonian systems. *Sci. Adv.* **5**, DOI: [10.1126/sciadv.aav2372](https://doi.org/10.1126/sciadv.aav2372) (2019).
11. Fixstars amplify. <https://amplify.fixstars.com/en/>. Accessed 22 January 2024.
12. Jiang, S., Britt, K. A., McCaskey, A. J., Humble, T. S. & Kais, S. Quantum annealing for prime factorization. *Sci. Rep.* **8**, DOI: [10.1038/s41598-018-36058-z](https://doi.org/10.1038/s41598-018-36058-z) (2018).
13. Matsumori, T., Taki, M. & Kadowaki, T. Application of qubo solver using black-box optimization to structural design for resonance avoidance. *Sci. Rep.* **12**, DOI: [10.1038/s41598-022-16149-8](https://doi.org/10.1038/s41598-022-16149-8) (2022).

14. Endo, K., Matsuda, Y., Tanaka, S. & Muramatsu, M. A phase-field model by an ising machine and its application to the phase-separation structure of a diblock polymer. *Sci. Rep.* **12**, DOI: [10.1038/s41598-022-14735-4](https://doi.org/10.1038/s41598-022-14735-4) (2022).
15. Wang, Y., Kim, J. E. & Suresh, K. Opportunities and challenges of quantum computing for engineering optimization. *J. Comput. Inf. Sci. Eng.* **23**, DOI: [10.1115/1.4062969](https://doi.org/10.1115/1.4062969) (2023).
16. Yarkoni, S., Raponi, E., Bäck, T. & Schmitt, S. Quantum annealing for industry applications: introduction and review. *Rep. Prog. Phys.* **85**, DOI: [10.1088/1361-6633/ac8c54](https://doi.org/10.1088/1361-6633/ac8c54) (2022).
17. Haftka, R. T. & Gürdal, Z. *Elements of structural optimization*, vol. 11 (Springer Science & Business Media, 2012).
18. Andreassen, E., Clausen, A., Schevenels, M., Lazarov, B. S. & Sigmund, O. Efficient topology optimization in matlab using 88 lines of code. *Struct. Multidiscip. Optim.* **43**, 1–16, DOI: [10.1007/s00158-010-0594-7](https://doi.org/10.1007/s00158-010-0594-7) (2011).
19. Bureerat, S. & Limtragool, J. Structural topology optimisation using simulated annealing with multiresolution design variables. *Finite Elem. Anal. Des.* **44**, 738–747, DOI: [10.1016/j.finel.2008.04.002](https://doi.org/10.1016/j.finel.2008.04.002) (2008).
20. Lamberti, L. An efficient simulated annealing algorithm for design optimization of truss structures. *Comput. & Struct.* **86**, 1936–1953, DOI: [10.1016/j.compstruc.2008.02.004](https://doi.org/10.1016/j.compstruc.2008.02.004) (2008).
21. Deb, K. & Gulati, S. Design of truss-structures for minimum weight using genetic algorithms. *Finite Elem. Anal. Des.* **37**, 447–465, DOI: [10.1016/S0168-874X\(00\)00057-3](https://doi.org/10.1016/S0168-874X(00)00057-3) (2001).
22. Wang, S. Y. & Tai, K. Structural topology design optimization using genetic algorithms with a bit-array representation. *Comput. Methods Appl. Mech. Eng.* **194**, 3749–3770, DOI: [10.1016/j.cma.2004.09.003](https://doi.org/10.1016/j.cma.2004.09.003) (2005).
23. Lee, K. S. & Geem, Z. W. A new structural optimization method based on the harmony search algorithm. *Comput. & Struct.* **82**, 781–798, DOI: [10.1016/j.compstruc.2004.01.002](https://doi.org/10.1016/j.compstruc.2004.01.002) (2004).
24. Xie, Y. M. & Steven, G. P. A simple evolutionary procedure for structural optimization. *Comput. & Struct.* **49**, 885–896, DOI: [10.1016/0045-7949\(93\)90035-C](https://doi.org/10.1016/0045-7949(93)90035-C) (1993).
25. Huang, X. & Xie, Y. M. Convergent and mesh-independent solutions for the bi-directional evolutionary structural optimization method. *Finite Elem. Anal. Des.* **43**, 1039–1049, DOI: [10.1016/j.finel.2007.06.006](https://doi.org/10.1016/j.finel.2007.06.006) (2007).
26. Wils, K. *Quantum Computing for Structural Optimization*. Master’s thesis, Delft University of Technology (2020).
27. Wils, K. & Chen, B. A symbolic approach to discrete structural optimization using quantum annealing. *Mathematics* **11**, 3451, DOI: [10.3390/math11163451](https://doi.org/10.3390/math11163451) (2023).
28. Sato, Y., Kondo, R., Koide, S. & Kajita, S. Quantum topology optimization of ground structures using noisy intermediate-scale quantum devices. Preprint at <https://arxiv.org/abs/2207.09181> (2022).
29. Sato, Y., Kondo, R., Koide, S. & Kajita, S. Quantum topology optimization of ground structures for near-term devices. *Proc. - 2023 IEEE Int. Conf. on Quantum Comput. Eng. QCE 2023* **1**, 168–176, DOI: [10.1109/QCE57702.2023.00027](https://doi.org/10.1109/QCE57702.2023.00027) (2023).
30. Ye, Z., Qian, X. & Pan, W. Quantum topology optimization via quantum annealing. *IEEE Trans. Quantum Eng.* **4**, DOI: [10.1109/TQE.2023.3266410](https://doi.org/10.1109/TQE.2023.3266410) (2023).
31. O’Malley, D. & Vesselinov, V. V. Toq.jl: A high-level programming language for d-wave machines based on julia. In *2016 IEEE High Performance Extreme Computing Conference (HPEC)*, 1–7, DOI: [10.1109/HPEC.2016.7761616](https://doi.org/10.1109/HPEC.2016.7761616) (Waltham, MA, USA, 2016).
32. Jun, K. Qubo formulations for a system of linear equations. *Results Control. Optim.* **14**, 100380, DOI: <https://doi.org/10.1016/j.rico.2024.100380> (2024).

Author contributions

N.S.: Optimization framework, Software, Validation, Investigation, Writing-original draft preparation; X.J. and K.W.: Quantum annealing discussion, Investigation, Review; S.M.: Investigation, Review-original draft; K.T.: Funding acquisition, Conceptualization, Methodology, Supervision, Writing- Reviewing and Editing.

Additional information

Competing interests The authors declare no competing interests.